

# Objective Determination of Star Formation Histories

Gerard Gilmore<sup>1</sup>, Xavier Hernandez<sup>1,2</sup>, & David Valls-Gabaud<sup>1,3</sup>

<sup>1</sup>*IoA Cambridge*, <sup>2</sup>*Arcetri Observatory*, <sup>3</sup>*CNRS, Toulouse Observatory*

**Abstract.** Objective determination of a star formation history from a colour-magnitude diagram, independently of assumed parametric descriptions, is necessary to determine the evolutionary history of a galaxy. We introduce a new method for solving maximum likelihood problems through variational calculus, and apply it to the case of recovering an unknown star formation history,  $SFR(t)$ , from a colour-magnitude diagram. This method provides a non-parametric solution with the advantage of requiring no initial assumptions on the  $SFR(t)$ . As a full maximum likelihood statistical model is used, one may exploit all the information available in the photometric data which can be explained by available isochrones. Extensive tests of the method show it to be reliable under noise conditions comparable to those appropriate for real observations. Implications for future surveys, such as the GAIA mission are significant: accurate determination of the evolutionary history of the Milky Way is limited only by adequate spectroscopy and/or photometry to provide a determination of stellar metallicity and temperature for a sufficient sample of stars of luminosities at and above an old main-sequence turnoff.

## 1. Introduction

A primary scientific goal in the quantification of galactic evolution is the derivation of the star formation histories, as described by the temporal evolution of the star formation rate,  $SFR(t)$ . In practice, uncertainties in the theories of stellar formation and evolution, as well as degeneracy between age and metallicity, not to mention observational errors and unknown distance and reddening corrections, make inferring  $SFR(t)$  for mixed stellar populations a difficult task. Even assuming a known stellar initial mass function ( $IMF$ ) and metallicity, a given set of isochrones and no distance or reddening uncertainties, recovering the  $SFR(t)$  which gave rise to a given stellar mix is not trivial.

The increasing application of HST studies which resolve the stellar populations of nearby systems has initiated quantitative investigation of the  $SFR(t)$  in these systems through the comparison of observed and synthetic colour-magnitude (C-M) diagrams (e.g. Chiosi et al. (1989), Aparicio et al. (1990) and Mould et al. (1997) using Magellanic and local clusters, and Mighell & Butcher (1992), Smecker-Hane et al. (1994), Tolstoy (1995), Aparicio & Gallart (1995) and Mighell (1997) using dSph companions to the Milky Way). These studies construct a statistical estimator to compare a synthetic C-M diagram constructed from an assumed  $SFR(t)$  with an observed one, and then select the



$SFR(t)$ , from amongst a set of plausible ones, which maximizes the value of this estimator (e.g. Tolstoy & Saha 1996). The most rigorous estimator is probably the likelihood, as defined through Bayes’s theorem. In practice this states that one should look for the model which maximizes the probability of the observed data set having arisen from it. The apparent robustness of the approach is undermined by the iagramsree of subjectivity associated with defining the set of plausible models one is able to consider. Further, as none of the statistical estimators has an absolute normalization, in the end one is left with that model, of the ones one started by proposing, which best reproduces the data. This best model is not necessarily a “good” approximation to the true  $SFR(t)$ . The likelihood of the data having arisen from a particular model can only be calculated if one has the data, the errors, and the particular model fully specified. This last condition has led to the almost exclusive use of parametric  $SFR(t)$  histories.

Presently, methods of comparing simulated C-M diagrams with observations can be classified according to the statistical criterion used in the comparison. A few examples of the variety in these categories are Tolstoy (1995) and Mould et al. (1997) who use full maximum likelihood statistics, Dolphin (1997) and Ng (1998) who use chi-squared statistics, and Aparicio et al. (1997) and Hurley-Keller et al. (1998) who break the C-M diagrams into luminosity functions before constructing the statistical estimator.

We (Hernandez, Valls-Gabaud & Gilmore 1999a,1999b; Hernandez, Gilmore & Valls-Gabaud 1999) have developed a variational calculus method of solving directly for the maximum likelihood  $SFR(t)$ , which does not require any assumptions on the function one is trying to recover, or to evaluate the likelihood of any of the  $SFR(t)$ ’s being considered (all continuous functions of time). We construct an integro-differential equation which is solved to find a  $SFR(t)$  which yields a vanishing first variation for the likelihood. At each iteration the  $SFR(t)$  is solved with an arbitrary time resolution. Conveniently, computation times scale only linearly with this time resolution. This allows a very detailed reconstruction of the  $SFR(t)$ , which would be prohibitively expensive in a parametric decomposition of the  $SFR(t)$ .

Full details of the model, the extensive tests and calibrations, and its application to new HST data for the Galactic dSph satellites, are presented in the references noted (Hernandez et al. 1999, 1999a, 1999b). In this paper we summarise the method and its validity, then simulate GAIA observations of an old metal-poor stellar population, a young metal rich population, and a mixed population. These simulations show that GAIA data can indeed meet the scientific goal required, quantify

the metallicity accuracy needed, and quantify the photometric precision required by GAIA at faint magnitudes.

## 2. Deriving star formation histories

Our goal is to recover the star formation history which gave rise to an observed population of stars, described by  $SFR(t)$ , the star formation rate as a function of time. For fully general applicability, we shall assume nothing about the  $SFR(t)$  we are trying to recover, except that it should be a continuous function of time. One general constraint will be the total number of stars produced, which provides the SFR normalisation condition, over the range of masses over which stars can be observed. In the general case, we are concerned only with that fraction of the total star formation which produced stars still readily observable today, which corresponds in external galaxies and at large distances in the Galaxy to masses greater than about 0.5 solar masses. We emphasise that this mass constraint is relevant only in that it must be lower than the oldest turnoff mass of relevance to the application at hand. Also note that this requires an accurate determination of the local completeness limit in any modelled data set, but does not imply that this completeness limit have a value near unity.

The final observed C-M diagrams as a function of place are the result of the star formation histories in those places, later dynamical evolution, and also of the relevant initial mass function, the metallicity and the stellar evolutionary processes. As we see later, it is essential that the IMF near the turnoff, and the star by star metallicity, be independently known. It is this requirement which is the primary science case for GAIA to determine stellar metallicity, and which constrains the requisite photometric performance. [Note that there are other astrophysical systems for which this essentially holds, and for which only the star formation history is poorly known. Examples of such systems are some of the dwarf spheroidal companions to our Galaxy, whose star formation histories we have derived.]

In the Milky Way, we are primarily interested in stars which are observable at the distance of the Galactic centre, and the stellar edge of the disk. This determines the mass regime over which the initial mass function needs to be well established. Theoretical studies of stellar isochrones have advanced significantly over the last decade, and now there seems to be little uncertainty in the physical properties of stars over the mass range 0.6–3 solar masses, during all but the shortest lived evolutionary periods. Here we are using the latest Padova isochrones (Fagotto et al. 1994, Girardi et al. 1996), including most stages of

stellar evolution up to the RGB phase. Our detailed inferences will depend on the precise details of the isochrones we use. Our aim here is not to insist upon any particular age calibration, and indeed any and all isochrones can be used. The key feature of this method is that it provides a robust and objective relative age ranking of the stellar population. The mapping of that age ranking onto an external time scale is isochrone-dependent, insofar as different isochrones do not (yet) all agree, but the relative distributions are robust.

## 2.1. THE METHOD

Consider a fixed set of observations  $A = (A_1, \dots, A_n)$ , which result from a model which belongs to a certain known set of models  $B = B_1, \dots$ . We want to identify the model which has the highest probability of generating the observed data set,  $A$ . That is, we wish to identify the model which maximizes  $P(AB_i)$ , the joint probability of  $A$  occurring for a given model  $B_i$ . From the definition of conditional probabilities,

$$P(AB_i) = P(A|B_i) \cdot P(B_i) = P(B_i|A) \cdot P(A) \quad (1)$$

where  $P(A|B_i)$  is the conditional probability of observing  $A$  given that a specific model  $B_i$  occurred,  $P(B_i|A)$  is the conditional probability of model  $B_i$  given the observed data  $A$ , and  $P(A), P(B_i)$  are the independent probabilities of  $A$  and  $B_i$ , respectively. Further, if the  $B_i$ s are exclusive and exhaustive,

$$P(A) = \int_i P(A|B_i) \cdot P(B_i) = 1/C \quad (2)$$

where  $C$  is a constant, so that equation (1) becomes:

$$P(B_i|A) = C \cdot P(A|B_i) \cdot P(B_i) \quad (3)$$

which is Bayes' theorem.  $P(B_i)$  is called the *prior* distribution, and defines what is known about model  $B_i$  without any knowledge of the data. As we want to maximize the importance of the data in our inference process, we adopt the hypothesis of equal prior probabilities. Finding the maximum likelihood model under this assumption is hence simplified to finding the model  $B_i$  for which  $P(A|B_i)$  is maximized. Our set of models from which the optimum  $SFR(t)$  is to be chosen includes all continuous, twice differentiable functions of time, with the external constraint that the total number of stars formed does not conflict with the observed C-M diagram.

In order to find the  $SFR(t)$  which maximizes the probability of the observed C-M diagram resulting from it, we first have to introduce

a statistical model to calculate the probability of the data resulting from a given  $SFR(t)$ . Consider one particular star, having an observed luminosity and colour,  $l_i, c_i$ , and an intrinsic luminosity and colour  $L_i, C_i$ , where the index  $1 < i < n$  distinguishes between the  $n$  observed stars making up the C-M diagram. The intrinsic and observed quantities will not be identical, due to observational errors. The probability of this observed point being a star actually described by a particular isochrone  $C(L; t_j)$ , i.e., being one of the stars formed at time  $t_j$  as part of the rate  $SFR(t_j)$ , will be given by:

$$P_i(t_j) = SFR(t_j) \frac{\rho(L_i; t_j)}{\sqrt{2\pi} \sigma(l_i)} \exp\left(\frac{-[C(L_i; t_j) - c_i]^2}{2 \sigma^2(l_i)}\right) \quad (4)$$

In equation (4)  $\sigma(l_i)$  denotes the observational error in the measurement of the colour of the  $i$ th observed star, which is a function of the luminosity of this star, and which we are assuming follows a Gaussian distribution. For simplicity here we only consider errors in colour, which increase with decreasing luminosity, in a way determined by the particular observation. In this case  $L_i = l_i$  which we adopt throughout, the generalization to an error ellipsoid being trivial.  $C(L_i; t_j)$  is the colour the observed star having luminosity  $l_i$  would have if it had actually formed at  $t = t_j$ .  $\rho(L_i; t_j)$  is the density of stars along the isochrone  $C(L; t_j)$  around the luminosity of the observed star,  $l_i$ , for an isochrone containing a unit total mass of stars. Therefore, for stars in their main sequence phase,  $\rho(L; t_j)$  is actually the initial mass function expressed in terms of the luminosity of the stars. Further along the isochrone it contains the initial mass function convolved with the appropriate evolutionary track. Finally,  $SFR(t_j)$  indicates the total mass of stars contained in the isochrone in question, and is the only quantity in equation (4) which we ignore, given an observational C-M diagram, an initial mass function and a continuous set of isochrones.

The probability of the observed point  $l_i, c_i$  being the result of a specific  $SFR(t)$  will therefore be:

$$P_i(SFR(t)) = \int_{t_0}^{t_1} SFR(t) G_i(t) dt \quad (5)$$

where

$$G_i(t) = \frac{\rho(L_i; t)}{\sqrt{2\pi} \sigma(l_i)} \exp\left(\frac{-[C(L_i; t) - c_i]^2}{2 \sigma^2(l_i)}\right)$$

and where  $t_0$  and  $t_1$  are a maximum and a minimum time needed to be considered in a specific astrophysical or observational situation. We shall refer to  $G_i(t)$  as the likelihood matrix. At this point we introduce

the hypothesis that the  $n$  different observed points making up the total C-M diagram are independent events, to construct:

$$\mathcal{L} = \prod_{i=1}^n \left( \int_{t_0}^{t_1} SFR(t) G_i(t) dt \right) \quad (6)$$

which is the probability that the full observed C-M diagram resulted from a given  $SFR(t)$ . The discussion to here is essentially a review, and can be found similarly in, e.g., Tolstoy & Saha (1996).

The remainder of the development is entirely new. We have used equation (6) to construct the Euler equation of the problem, and hence obtain an integro-differential equation directly for the maximum likelihood  $SFR(t)$ , independent of *a priori* assumptions. It is the functional  $\mathcal{L}(SFR(t))$  which we want to maximize with respect to  $SFR(t)$  to find the maximum likelihood star formation history.

The condition that  $\mathcal{L}(SFR)$  has an extremal can be written as

$$\delta \mathcal{L}(SFR) = 0,$$

and the techniques of variational calculus brought to bear on the problem. Firstly, we develop the product over  $i$  using the chain rule for the variational derivative, and divide the resulting sum by  $\mathcal{L}$  to obtain:

$$\sum_{i=1}^n \left( \frac{\delta \int_{t_0}^{t_1} SFR(t) G_i(t) dt}{\int_{t_0}^{t_1} SFR(t) G_i(t) dt} \right) = 0 \quad (7)$$

In order to construct an integro-differential equation for  $SFR(t)$  we introduce the new variable  $Y(t)$  defined as:

$$Y(t) = \int \sqrt{SFR(t)} dt \implies SFR(t) = \left( \frac{dY(t)}{dt} \right)^2$$

Introducing the above expression into equation (7) and developing the Euler equation yields,

$$\frac{d^2 Y(t)}{dt^2} \sum_{i=1}^n \left( \frac{G_i(t)}{I(i)} \right) = - \frac{dY(t)}{dt} \sum_{i=1}^n \left( \frac{dG_i/dt}{I(i)} \right) \quad (8)$$

where

$$I(i) = \int_{t_0}^{t_1} SFR(t) G_i(t) dt$$

We have thus constructed an integro-differential equation whose solution yields a  $SFR(t)$  for which the likelihood has a vanishing first variation. This in effect has transformed the problem from one of searching for a function which maximizes a product of integrals (equation 6)

to one of solving an integro-differential equation (equation 8). Solving equation (8) will be the main problem, as this would yield the required star formation history directly, without having to calculate  $\mathcal{L}$  explicitly over the whole functional space containing all the possible  $SFR(t)$ s.

One may now implement an iterative scheme for solving equation(8), the details of which are given in Hernandez, Valls-Gabaud & Gilmore (1999). Given the complexity of the isochrones, the initial mass function and the unknown star formation histories we are trying to recover, it is not possible to prove convergence analytically for the implemented iterative method. Hernandez et al. show that the method works remarkably well for a wide range of synthetic C-M diagrams produced from known  $SFR(t)$ 's, independent of the initialisation used.

## 2.2. NUMERICAL IMPLEMENTATION

An important point of implementation, rather than general principle, involves calculation of the isochrones. To produce a realistic C-M diagram from a proposed  $SFR(t)$  requires firstly a method of obtaining the colour and luminosity of a star of a given mass and age. Interpolating between isochrones is a risky procedure which can imprint spurious structure in the inference procedure, given the almost discontinuous way in which stellar properties vary across critical points along the isochrones, and how these critical points vary with time and metallicity.

To avoid this we use the latest Padova (Fagotto et al. 1994, Girardi et al. 1996) full stellar tracks, calculated at fine variable time intervals, and a careful interpolating method which uses only stars at constant evolutionary phases to construct an isochrone library. We calculate 100 isochrones containing 1000 uniformly spaced masses each, with a linear spacing between 0.1 and 15 Gyr, which determines the time resolution with which we implement the method to be 150 Myr. An arbitrary time resolution can be achieved using a finer isochrone grid, which increases the calculation times only linearly with the number of intervals.

Having fixed the isochrones, we now need to specify the manner in which the density of stars will vary along these isochrones, i.e. an IMF. We use the IMF derived by Kroupa et al. (1993), where a single fit to this function is seen to hold for stars towards both Galactic poles, and for all stars in the solar neighbourhood. In analyzing the stellar distribution towards the Galactic poles, a wide range of metallicities and ages is sampled, and care was taken to account for all the effects this introduces, including the changing mass-luminosity relation at different ages and metallicities, completeness effects as a function of luminosity and distance, and the contribution of binaries.

We normalise the mass distribution such that a unit total mass is contained upwards of  $0.08M_{\odot}$ , although only stars in the mass range  $0.6 - 3M_{\odot}$  can end up in the C-M diagram. We can now choose a  $SFR(t)$ , and use the IMF to populate our isochrones and create a synthetic C-M diagram, after including “observational” errors, assumed to be Gaussian-distributed on  $\log(T)$ .

It is worth noting that the slope of the low-mass IMF,  $-1.3$ , is in exact agreement with the one derived from very recent studies of metal-poor globular clusters, and the UMi dwarf spheroidal galaxy, in both cases from very deep HST data. It thus seems well-established.

### 3. Testing the method: a summary

To illustrate the validity of the method, we present here a small subset of the simulation results of Hernandez et al., where further details may be found. The method used here is to create an artificial colour-magnitude diagram from a set of adopted star formation histories, and then to apply the method above to deduce a star formation history from the CMD. The true simulation input and the derived output are compared, the insensitivity to assumed star formation histories is apparent, the reliability of the method is illustrated, while the extreme age-metallicity degeneracy which irreducibly affects any analysis of stellar photometric data is explored.

#### 3.1. A SIMPLE TWO-BURST EXAMPLE

As a first test we use a  $SFR(t)$  consisting of two Gaussian bursts at different epochs, of different amplitudes and total masses. This  $SFR(t)$  is shown by the dashed line in the right panel of Figure (1), where the time axis shows the age of the corresponding stellar populations. The left panel of Figure (1) shows the resulting C-M diagram which contains a total of 3819 stars. A realistic error structure was applied, from actual HST observations.

The calculation proceeds using the stars with  $\log(L) > 0$  in Figure (1), from which we construct the matrix  $G_i(t)$ . Since the colour of a star having a given luminosity can sometimes be a multi-valued function, in practice we check along a given isochrone, to find all possible masses a given observed star might have as a function of time, and add all contributions (mostly 1, sometimes 2 and occasionally 3) in the same  $G_i(t)$ . Calculating this matrix is the only slow part of the procedure, and is equivalent to calculating the likelihood of one model. The likelihood matrix  $G_i(t)$  is the only input required by the numerical



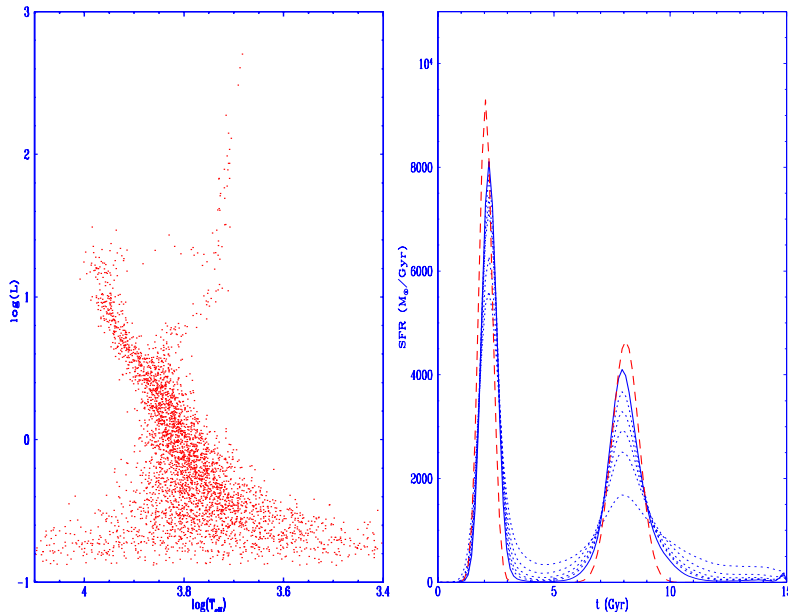


Figure 1. Left: Synthetic C-M diagram resulting from a simple two-burst input  $SFR(t)$ . Right: Input  $SFR(t)$ , dashed line. Also shown are the 3, 6, 9, 12 and 15 iterations of the inversion method, as dotted curves. The 20th iteration is given by the solid curve, showing the convergence and a reliable reconstruction of the input  $SFR(t)$ .

implementation. The total number of stars is used as a normalisation constraint at each iteration, needed to recover  $SFR(t)$  from  $Y(t)$ . As mentioned earlier, it is not necessary to calculate the likelihood over the solution space being considered, i.e.  $G_i(t)$  is only calculated once, which makes the method highly efficient.

In Figure (1) we also show the results of the first 12 iterations of the method every 2 iterations, which form a sequence of increasing resemblance to the input  $SFR(t)$ . The distance between successive iterations decreases monotonically at all ages, which together with the fact that after 12 iterations no further change is seen, shows the convergence of the method for this case. From the 2nd iteration (lowest dotted curve in the burst regions) it can be seen that the iteration of the variational calculus equation constructed from maximizing the likelihood is able to recover the input  $SFR(t)$  efficiently. The positions, shapes and relative masses of the two bursts were correctly inferred by the 2nd iteration, although it took longer for the method to eliminate the populations outside of the two input bursts. The convergence solution is in remark-

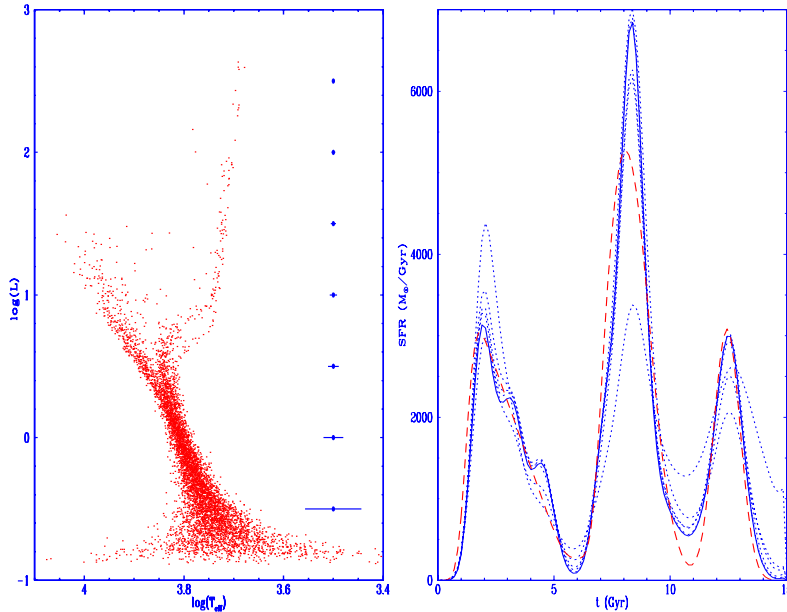


Figure 2. Left: A synthetic C-M diagram with smaller photometric errors. Right: The input  $SFR(t)$  is shown as a dashed line. Also shown are the 2, 4, 6, 8 and 9 iterations of the inversion method, dotted curves. The 10th iteration is given by the solid curve, showing rapid convergence and a good recovery of the input  $SFR(t)$ .

able agreement with the input  $SFR(t)$ , and only differs slightly, as seen from Figure (1). No information was used in the inverting procedure beyond that which is available from the synthetic C-M diagram, which was used extensively in constructing the likelihood matrix  $G_i(t)$ , which is the only input required by the inversion. The variational calculus method recovers a  $SFR(t)$  for which the first variation of the likelihood vanishes, without assuming any *a priori* condition on the  $SFR(t)$ , beyond being a continuous twice differentiable function of time.

### 3.2. VERY OLD POPULATIONS: SENSITIVITY TO PHOTOMETRIC ERRORS

Given that the method is now seen to work, how well can it work? The hardest case is for very old stars, where the colour-sensitivity to age differences is small. For this experiment we consider data of somewhat higher photometric precision that are routinely obtained with HST, but are similar to those from large ground-based and future space CCD arrays. Figure (2) has the same structure as Figure 1 above.

The data quality is reflected in the clearer C-M diagram, where the older population is distinguishable from the noise of the younger main sequence. The right panel in Figure (2) shows the result of the inversion procedure, and the rapidity of convergence, with only 10 iterations needed. The few stars in the oldest component which can be separated from the younger main sequence are sufficient to accurately recover the shape for this burst. That is, the method is able to deduce all the information present in the data.

### 3.3. SENSITIVITY TO UNCERTAINTIES IN IMF, METALLICITY AND BINARIES

Uncertainties in the IMF, metallicity and binaries differ from simple sample size or photometric error in inducing a systematic mismatch between the isochrones used in any specific calculation and those which describe the astrophysics of the C-M diagram being inverted. Of these effects, by far the most significant is the well known age-metallicity degeneracy, which implies that a reliable knowledge of the abundance distribution of the stars in the sample is essential for any reliable determination of age from photometric data.

We therefore consider the following test, where the C-M diagram is produced using a range of metallicities, and inverted assuming a single metallicity. This is presented in Figure (3) with a C-M diagram which results from a gaussian  $SFR(t)$ , where metallicity is not a delta function. In this case we assigned a metallicity of  $[Fe/H] = -1.7$  to stars older than 7.5 Gyr, and  $[Fe/H] = -0.7$  to stars younger than 7.5 Gyr, i.e., a crude enrichment history. This is clearly seen in Figure (3, LHS), where the two populations having different metallicities are evident, from the width of the RGB. The noise level is the same as in Figure (1). The result of applying the inversion method assuming a single metallicity of  $[Fe/H] = -1.7$  is shown in the right panel of Figure (3). The method correctly identifies the half of the  $SFR(t)$  with the lower metallicity; the higher metallicity population is totally misinterpreted. Actually, the age the inversion procedure should assign to the high metallicity component is in fact greater than 15 Gyr, which is in contradiction with the fixed boundary condition of  $SFR(15) = 0$ . This makes the inversion procedure somewhat unstable, which in principle can be used to indicate that the isochrones being used in the inversion procedure do not correspond to the studied stars. The two distinct giant branches seen in this C-M diagram indicate a difference in the metallicities of both populations.

As it might have been expected, uncertainties in the metallicity distort the inference procedure significantly, making the determina-

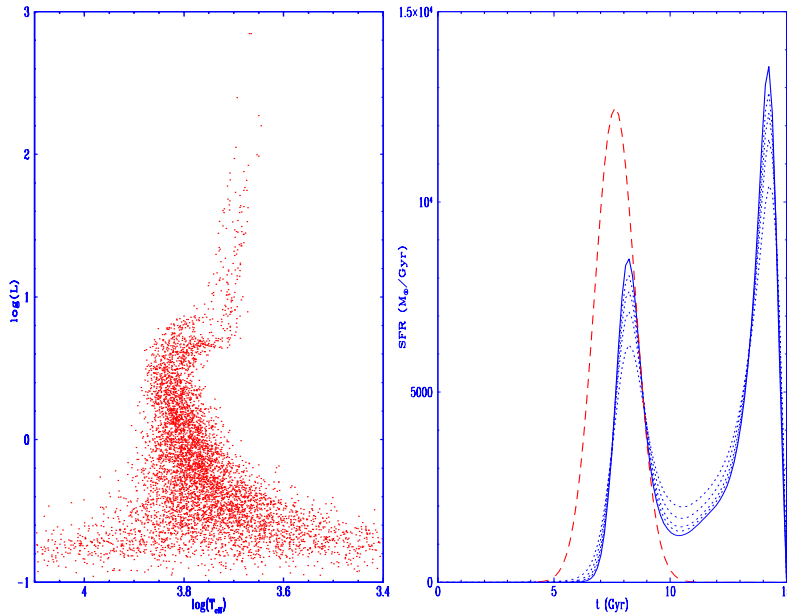


Figure 3. Left: Synthetic C-M diagram produced using a metallicity of  $[Fe/H] = -1.7$  for the stars older than 7.5 Gyr and of  $[Fe/H] = -0.7$  for the stars younger than 7.5 Gyr. Right: The input  $SFR(t)$  is shown as the dashed line. Also shown are the 3, 6, 9, 12 and 15 iterations of the inversion method (dotted curves) assuming a (wrong) constant metallicity ( $[Fe/H] = -1.7$ ) for the entire evolution, which confuses the method. The 18th iteration is given by the solid curve.

tion of star formation histories robust only in cases where individual metallicities are available.

#### 4. Conclusions concerning the method

We can summarize our methodological results as follows:

1) We have introduced a variational calculus scheme for solving maximum likelihood problems, and tested it successfully in the particular case of inverting C-M diagrams.

2) Assuming a known IMF and metallicity we have presented a non-parametric method for inverting C-M diagrams which yields good results when recovering stellar populations younger than 10 Gyr, with data quality similar to those attained in current HST observations of dSph galaxies. Populations older than 10 Gyr can only be recovered equally well from C-M diagrams with much reduced observational errors, compared to current HST performance.

3) Uncertainties in the IMF and binary fractions result in normalisation errors on the total  $SFR(t)$ . Given the existence of an age-metallicity degeneracy on the colours and magnitudes of stars, an error in the assumed metallicity results in a seriously mistaken  $SFR(t)$ . This makes the version of the variational calculus approach we present here useful only in cases where the metallicity of the stars is knowable independently of the form of the colour-magnitude diagram near the turnoff.

4) The main-sequence turnoff of the oldest stellar populations corresponds to apparent magnitude  $\sim 20$  at the Galactic centre, and near the apparent outer edge of the disk. GAIA can therefore determine the full star formation history of the near half of the Milky Way for all ages. This provides a sufficiently large sample that the global star formation history of our Galaxy can indeed be determined by GAIA. The star formation history at more recent times can also be determined for larger distances, especially in the Magellanic Clouds and the Sgr dSph. Such determinations however require metallicity measures accurate to about 0.2 dex, and photometric data able to provide stellar effective temperatures good to about 10% of  $T_{\text{eff}}$ , for stars at and above the turnoff.

## References

- Aparicio A., Bertelli G., Chiosi C., Garcia-Pelayo J.M., 1990, A&A 240, 262  
 Aparicio A., Gallart C., 1995, AJ, 110, 2105  
 Aparicio A., Gallart C., Bertelli G., 1997, AJ, 114, 669  
 Chiosi C., Bertelli G., Meylan G., Ortolani S., 1989, A&A, 219, 167  
 Dolphin A., 1997, New Astronomy, 2, 397  
 Fagotto F., Bressan A., Bertelli G., Chiosi C., 1994, A&AS, 104, 365  
 Girardi L., Bressan A., Chiosi C., Bertelli G., Nasi E., 1996, A&AS 117, 113  
 Hernandez, X., Valls-Gabaud, D., & Gilmore, G., 1999 MNRAS 304, 705  
 Hernandez, X., Gilmore, G. & Valls-Gabaud, D., 1999 MNRAS in press  
 Hernandez, X., Valls-Gabaud, D., & Gilmore, G., 1999 MNRAS submitted  
 Hurley-Keller D., Mateo M., Nemej J., 1998, AJ, 115, 1840  
 Kroupa P., Tout C.A., Gilmore G., 1993, MNRAS, 262, 545  
 Mighell K.J., Butcher H.R., 1992, A&A, 255, 26  
 Mighell K.J., 1997, AJ, 114, 1458  
 Mould J.R., Han M., Stetson P.B., et al., 1997, ApJ, 483, L41  
 Ng Y.K., 1998, A&AS, 132, 133  
 Smecker-Hane T.A., Stetson P.B., Hesser J.E., Lehnert M.D., 1994, AJ, 108, 507  
 Tolstoy E., 1995, PhD. Thesis, Groeningen University, The Netherlands.  
 Tolstoy E., Saha A., 1996, ApJ, 462, 672

